Heliyon 10 (2024) e34403

Contents lists available at ScienceDirect

Heliyon

journal homepage: www.cell.com/heliyon

Research article

Development and validation of prognostic signatures of NAD+ metabolism and immune-related genes in colorectal cancer

Tao Ye [a,1], Hong Huang [b,1], Kangli Chen [b], Yuanao Yu [b], Dongqin Yue [b], Li Jiang [b], Huixian Wu [b], Ning Zhang [c,*]

[a] Department of Rehabilitation, The First Affiliated Hospital of Guizhou University of Traditional Chinese Medicine, Guiyang 550001, Guizhou, China
[b] The First Clinical College of Guizhou University of Traditional Chinese Medicine, Guiyang 550001, Guizhou, China
[c] Department of Pharmacy, The First Affiliated Hospital of Guizhou University of Traditional Chinese Medicine, Guiyang 550001, Guizhou, China

ARTICLE INFO

Keywords:
Colorectal cancer
NAD+ metabolism-related genes
Immune-related genes
Prognostic signature

ABSTRACT

Background: Colorectal cancer (CRC) is a prevalent cause of death from malignant tumors. This study aimed to develop a nicotinamide adenine dinucleotide (NAD+) metabolism and immune-related prognostic signature, providing a theoretical foundation for prognosis and therapy in CRC patients.

Methods: NAD + metabolism-related and immune-related subtypes of CRC patients were identified by consistent clustering. Differentially expressed genes (DEGs) between the two subtypes of CRC were identified by overlapping. A risk signature was constructed using univariate Cox and least absolute shrinkage and selection operator (LASSO) regression analyses. Independent prognostic predictors were authenticated by Cox analysis. Gene set variation analysis (GSVA) and single-sample gene set enrichment analysis (ssGSEA) were applied to investigate the connection between the prognostic signature and the immune microenvironment. Chemotherapy drug sensitivity and immunotherapy responsiveness were projected using the 'pRRophetic' package and Tumor Immune Dysfunction and Exclusion (TIDE) website. The Human Protein Atlas (HPA) database was used to assess the protein expression of prognostic genes in CRC and normal tissues.

Results: Using bioinformatics methods, three prognostic genes related to immune-related NAD + metabolism were identified, and the results were used to establish and verify a prognostic signature related to immune-related NAD + metabolism in CRC patients. Cox regression analysis confirmed that the risk score was a reliable independent prognostic predictor. GSVA and ssGSEA indicated that the prognostic signature was associated with the immune microenvironment. TIDE analysis suggested that the signature might act as an immunotherapy predictor. Chemotherapy sensitivity analysis revealed that *COMP* was correlated with chemotherapy sensitivity in CRC patients and might be a potential therapeutic target.

Conclusion: This study identified NAD + metabolism-immune-related prognostic genes (*MOGAT2*, *COMP*, and *DNASE1L3*) and developed a prognostic signature for CRC prognosis, which is significant for clinical prognosis prediction and treatment strategy decisions for CRC patients.

* Corresponding author. Department of Pharmacy, The First Affiliated Hospital of Guizhou University of Traditional Chinese Medicine; No.71, Baoshan North Road, Yunyan District, Guiyang City, Guizhou Province, 550001, China.
E-mail address: znzyyfy@163.com (N. Zhang).

[1] Tao Ye and Hong Huang have contributed equally to this work.

https://doi.org/10.1016/j.heliyon.2024.e34403
Received 27 November 2023; Received in revised form 1 July 2024; Accepted 9 July 2024
Available online 14 July 2024

1. Introduction

Colorectal cancer (CRC) is a prevalent malignant tumor globally and ranks as the second leading cause of cancer-related deaths. Its incidence and mortality rates continue to rise each year [1]. The most commonly observed type is adenocarcinoma, with squamous cell carcinoma, adenosquamous carcinoma, spindle cell carcinoma, and undifferentiated carcinoma occurring less frequently [2]. The primary treatment approaches for CRC include preoperative chemoradiotherapy or combined radiotherapy and chemotherapy following radical surgery in the early stages, chemotherapy in tandem with targeted therapy or immunotherapy in the middle and late stages, or neoadjuvant therapy [3]. Nonetheless, the overall survival rate for CRC patients remains considerably low, primarily due to tumor progression involving invasion and metastasis. With advancements in biotechnology, biomarkers can be employed to guide prognosis and treatment decisions, facilitating tailored treatment options to enhance patients' quality of life [4]. Consequently, early diagnosis and intervention play a pivotal role in reducing the incidence rate and improving the cure rate. Therefore, the identification of novel prognostic markers and models is of utmost importance. This is not only critical for improving patient prognosis but also crucial for providing patients with accurate treatment strategies.

Nicotinamide adenine dinucleotide [5] is an important metabolite and coenzyme that facilitates redox reactions in various metabolic pathways and cellular processes. It plays a central role in energy metabolism [6]. Studies have indicated that increased levels of NAD in CRC tissue can reduce reactive oxygen species levels, maintain cell stemness, and decrease the sensitivity of CRC cells to chemotherapy, thus impacting tumor growth [7]. Furthermore, NAD anabolism can enhance aging-associated secretory phenotypes, which in turn promote breast tumorigenesis [8]. In terms of tumor immunotherapy, nicotinamide adenine dinucleotide (NAD+) metabolism helps maintain inducible PD-L1 expression, drives tumor immune evasion, and sustains the activity and expression of the methylcytosine dioxygenase Tet1, mainly through α-ketoglutarate (α-KG). This ultimately reduces resistance to anti-PD-L1 antibody immunosuppressants [9]. Consequently, further exploration of the role of NAD + -related genes in the occurrence and progression of CRC is needed.

The immune system plays a crucial role in recognizing and eliminating tumors. The development, recurrence, and metastasis of tumors are closely associated with immune dysfunction, particularly abnormalities in cellular immune function, in which T cells are key players. Colorectal carcinogenesis is influenced by genetic and epigenetic alterations in tumor cells, as well as tumor-host interactions. Notably, robust lymphocyte responses observed in CRC tissues, characterized by high densities of $CD3^+$ T cells and T-cell subsets, are frequently associated with positive clinical results. This finding underscores the central role of T-cell-mediated immunity in suppressing tumor progression [10,11]. Additionally, a study [12] demonstrated that the abundance of tumor-infiltrating T cells correlated with specific molecular features of CRC. However, the association between NAD + -related genes and tumor immunity in the occurrence and progression of CRC requires further investigation.

To address these gaps in knowledge, this study used bioinformatics methods to identify NAD + metabolism- and immune-related subtypes in CRC patients. Subsequently, prognostic features related to NAD + metabolism and immunity were developed for CRC patients, with the aim of predicting patient prognosis and informing clinical treatment decisions. These findings offer insights into the associations among NAD + metabolism, immunity, and the mechanisms influencing the occurrence and progression of CRC.

2. Materials and methods

2.1. Dataset and gene source

We integrated transcriptomic data and clinical information from The Cancer Genome Atlas-Colorectal Cancer (TCGA-CRC) dataset, which consisted of 380 CRC tissue samples and 51 normal tissue samples. This integration was carried out using the UCSC database (http://xena.ucsc.edu/). Among these samples, 372 CRC samples were included in consensus clustering and survival analysis because they contained complete survival time records. In addition, we used two additional CRC datasets, GSE17538 and GSE115261, which were extracted from the Gene Expression Omnibus (GEO) database (https://www.ncbi.nlm.nih.gov/geo/). The GSE17538 dataset, which included 232 CRC samples with survival information, was used to validate our prognostic signature. The GSE115261 dataset, consisting of transcriptomic data from 10 CRC samples and 10 normal samples, was utilized for the validation of the expression of prognostic genes.

To identify NAD + metabolism-related genes (NMRGs), we mined data from the Kyoto Encyclopedia of Genes and Genomes (KEGG) pathway database (pathway: hsa00760, Nicotinate and nicotinamide metabolism) (https://www.genome.jp/kegg/pathway.html) and the Reactome database (pathway: R-HSA-196807, Nicotinate metabolism) (https://reactome.org/). Immune-related genes (IRGs) were identified from the ImmPort database (https://immport.niaid.nih.gov).

2.2. Consensus clustering

For consensus clustering, we used the 'ConsensusClusterPlus' package [13] to classify the 372 CRC patients in the TCGA-CRC cohort based on the expression of NMRGs or IRGs. The parameters were set as follows: maxK = 6, reps = 1000, pItem = 0.8, clusterAlg = 'pam', distance = 'canberra', and innerLinkage = 'complete'.

2.3. Identification of differentially expressed genes (DEGs)

We identified the differentially expressed genes (DEGs) through the 'limma' package (version 3.48.3 [14] based on the following threshold values: p value < 0.05 and $|\log_2\text{FoldChange}| > 1$.

2.4. Functional annotation analysis

We used the R package 'clusterProfiler' (version 4.0.5) [15] for Gene Ontology (GO) and KEGG enrichment analysis. GO terms were categorized into cellular component [3], molecular function (MF), and biological process (BP) terms. The significance criterion was an adjusted p value ≤ 0.05.

2.5. Creation of a prognostic signature related to immune-related NAD + metabolism in CRC

The TCGA-CRC dataset included a total of 372 patients whose survival information was available. Through randomization (ratio 7:3), the data were divided into a training set (n = 261) and a testing set (n = 111). In the training set, we performed univariate Cox analysis using the 'survminer' package (version 0.4.9) and least absolute shrinkage and selection operator (LASSO) regression analysis using the 'glmnet' package (version 4.0–2) to identify NAD + metabolism-immune-relevant prognostic genes. The RiskScore = $\sum_1^n \text{coef}(\text{genei}) \times \text{expression}(\text{genei})$ formula was used to separate patients into high-risk and low-risk subgroups based on the coefficient obtained by LASSO and the optimal threshold calculated using the surv_cutpoint function. We evaluated the predictive efficiency of the prognostic signature by analyzing Kaplan–Meier (K–M) curves, Receiver Operating Characteristic (ROC) analysis, and risk curves.

2.6. Relevance analysis of the gene signature and clinical parameters

Risk scores for the different clinical feature subgroups were compared with the Wilcoxon test (two groups) or Kruskal–Wallis test (more than two groups).

2.7. Independent prognostic analysis and nomogram construction

Risk score and clinical characteristic factors were included in the Cox analysis (univariate Cox and multivariate Cox) to determine independent prognostic predictors. A nomogram integrating the independent prognostic predictors was constructed using the R language 'rms' to predict survival at 1, 3 and 5 years in CRC patients. The calibration curves were employed to assess the precision of the prediction.

2.8. Correlation analysis of the prognostic signature and tumor immunity

The scores of the 13 immune-related pathways in the two risk subgroups were calculated by the gene set variation analysis (GSVA) algorithm [16]. The scores of 24 types of infiltrating immune cells for each sample in the two risk subgroups were assessed by the single-sample gene set enrichment analysis (ssGSEA) algorithm [17]. The correlation between prognostic genes and immune cells was measured through the TIMER database (https://cistrome.shinyapps.io/timer/).

2.9. Therapy analysis based on the prognostic signature

We inferred and assessed the sensitivity of the two risk subgroups to immune checkpoint inhibitor [18] therapy using the TIDE algorithm [19]. Furthermore, using the 'pRRophetic' R package [20], we computed the half maximal inhibitory concentration (IC_{50}) values for each patient in the two risk subgroups to analyze the correlation between prognostic genes and chemotherapy drug sensitivity.

Table 1
Primer sequences for qPCR.

Primer	Sequences
MOGAT2 For	CTGTTACTGCGGAACCGAAAG
MOGAT2 Rev	CCATGAAAGAGTGGGAGGGAG
DNASE1L3 For	CGTGAAACACCGCTGGAAGG
DNASE1L3 Rev	TTGGGAACAACAGAACTGACGATT
COMP For	CCGAGTCCGCTGTATCAACA
COMP Rev	TATGTTGCCCGGTCTCACAC
GAPDH For	CCCATCACCATCTTCCAGG
GAPDH Rev	CATCACGCCACAGTTTCCC

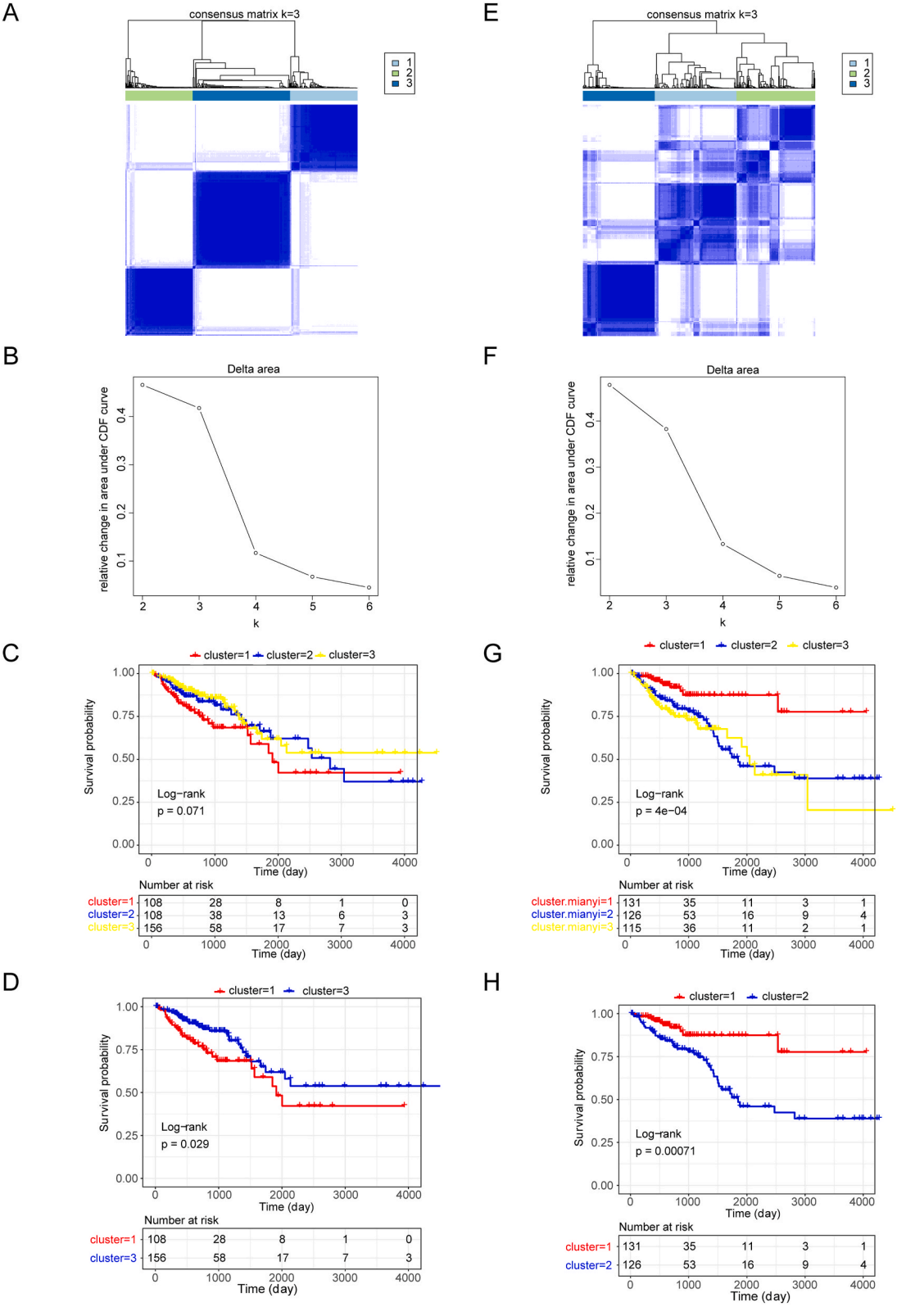

(caption on next page)

Fig. 1. Recognition of nicotinamide adenine dinucleotide (NAD+) metabolism-related and immune-related subtypes of colorectal cancer (CRC). (A) Consensus matrix heatmap depicting consensus values for each cluster (k) for NAD + metabolism-related subtypes. Clustering according to a consensus at K = 3. (B) Delta area plot reflecting the relative changes in the area under the cumulative distribution function (CDF) curve for the NAD + metabolism-related subtypes. (C) Survival curves of CRC patients with three clusters of NAD + metabolism-related subtypes. (D) Survival curves of patients with CRC stratified according to the NAD + metabolism-related subtypes in cluster 1 and cluster 3. (E) Consensus matrix heatmap depicting consensus values for each cluster (k) for immune-related subtypes. Clustering according to a consensus at K = 3. (F) Delta area plot reflecting the relative changes in the area under the CDF curve for immune-related subtypes. (G) Survival curves of CRC patients with three clusters of immune-related subtypes. (H) Survival curves of CRC patients with immune-related subtypes in cluster 1 and cluster 2.

2.10. Analysis and verification of the expression of prognostic genes

We initially observed a discrepancy in the expression of prognostic genes in CRC and normal samples in the external dataset GSE115261. Box-line plots illustrating this discrepancy were created using the 'ggpubr' package (version 0.4.0). To further determine the protein expression levels of prognostic genes in normal and CRC tissues, we utilized immunohistochemistry images from the Human Protein Atlas (HPA) database. We obtained human normal colonic epithelial cells (CCD814) and three human CRC cell lines (HCT-116, LOVO, and SW480) from iCell Bioscience, Inc. (Shanghai, China). The cells were incubated at 37 °C in an atmosphere of 5 % CO_2. Total RNA was extracted from the four cell lines in the logarithmic growth phase using TRIzol Reagent following the instructions from Ambion (USA). Total RNA was then reverse transcribed into cDNA using the SweScript First-Strand cDNA Synthesis Kit from Servicebio (China). qPCR was subsequently performed using 2 × Universal Blue SYBR Green qPCR Master Mix according to the manufacturer's directions (Servicebio, China). The sequences of primers used for qPCR are displayed in Table 1. The expression levels were normalized to those of the internal reference gene GAPDH and calculated using the $2^{-\Delta\Delta Ct}$ method [21].

2.11. Statistical analysis

A Venn diagram was generated using the Jvenn website (http://jvenn.toulouse.inra.fr/app/example.html) [22]. All bioinformatics analyses were performed using R language. The Wilcoxon test (for two groups) or Kruskal–Wallis test (for more than two groups) was used to compare the data from different groups.

3. Results

3.1. Recognition of NAD + metabolism-related and immune-related subtypes of CRC

Based on the expression of 35 NMRGs (Supplementary Table 1) detected in the TCGA-CRC dataset, we categorized the 372 CRC patients in the TCGA-CRC dataset into three NAD + metabolism-related subtypes through consensus clustering Fig. 1A and B). Survival analysis revealed significant differences in survival between cluster 1 and cluster 3 (p *value* = 0.029) (Fig. 1C and D). Furthermore, we classified these 372 CRC patients into three immune-related subtypes based on the expression of 1057 IRGs detected in the TCGA-CRC dataset (Fig. 1E and F). K–M curves revealed significant differences in survival between the three immune-related subtypes, with more pronounced survival disparities between cluster 1 and cluster 2 (p *value* = 0.00071) (Fig. 1G and H).

3.2. Identification of NAD + metabolism- and immune-related DEGs

Hence, we identified 55 DEGs between NAD + metabolism-related cluster 3 and cluster 1 (cluster 3 *vs* cluster 1). Among these DEGs, 2 genes were upregulated and 53 genes were downregulated in cluster 3 at the expression level Fig. 2A and B). Moreover, we discovered 706 DEGs between immune-related cluster 2 and cluster 1 (cluster 2 *vs* cluster 1). These DEGs consisted of 49 upregulated genes and 657 downregulated genes in cluster 2 Fig. 2C and D). Furthermore, we identified 4795 DEGs between CRC and normal samples in the TCGA-CRC dataset (tumor *vs* normal). Among these DEGs, 1577 genes were upregulated, and 3218 genes were downregulated (Fig. 2E and F). By intersecting these three sets of DEGs, we obtained 36 common genes related to NAD + metabolism and immune function (Fig. 2G–Table 2).

To investigate the functions of these 36 genes, we performed functional enrichment analysis. Tables 3 and 4 revealed 48 GO terms (21 BP terms, 11 CC terms, and 16 MF terms) and 3 KEGG pathways. We visualized the top 5 items for each GO category in a bubble diagram (Fig. 2H). GO analysis indicated that these genes are involved in immune-related processes, ion transport, digestion, and glycosylation (Fig. 2H–Table 3). KEGG pathway analysis revealed the involvement of these genes in "pancreatic secretion," "nitrogen metabolism," and "fat digestion and absorption" Fig. 2I–Table 4).

3.3. The NAD + metabolism-immune-related prognostic signature for CRC

To identify NAD + metabolism-immune-related genes associated with the overall survival (OS) of CRC patients, we conducted univariate Cox analysis using the 36 genes in the training set. Four genes were found to be significantly associated with OS in CRC patients (p value < 0.05). Among these genes, *COMP* was identified as a risk factor for CRC prognosis (hazard ratio (HR) > 1), whereas *MOGAT2*, *DNASE1L3*, and CEACAM7 were protective factors (HR < 1) (Fig. 3A). The four genes were further analyzed using LASSO analysis. Fig. 3B and C demonstrates that when the lambda min was 0.01, the optimal number of genes determined was three.

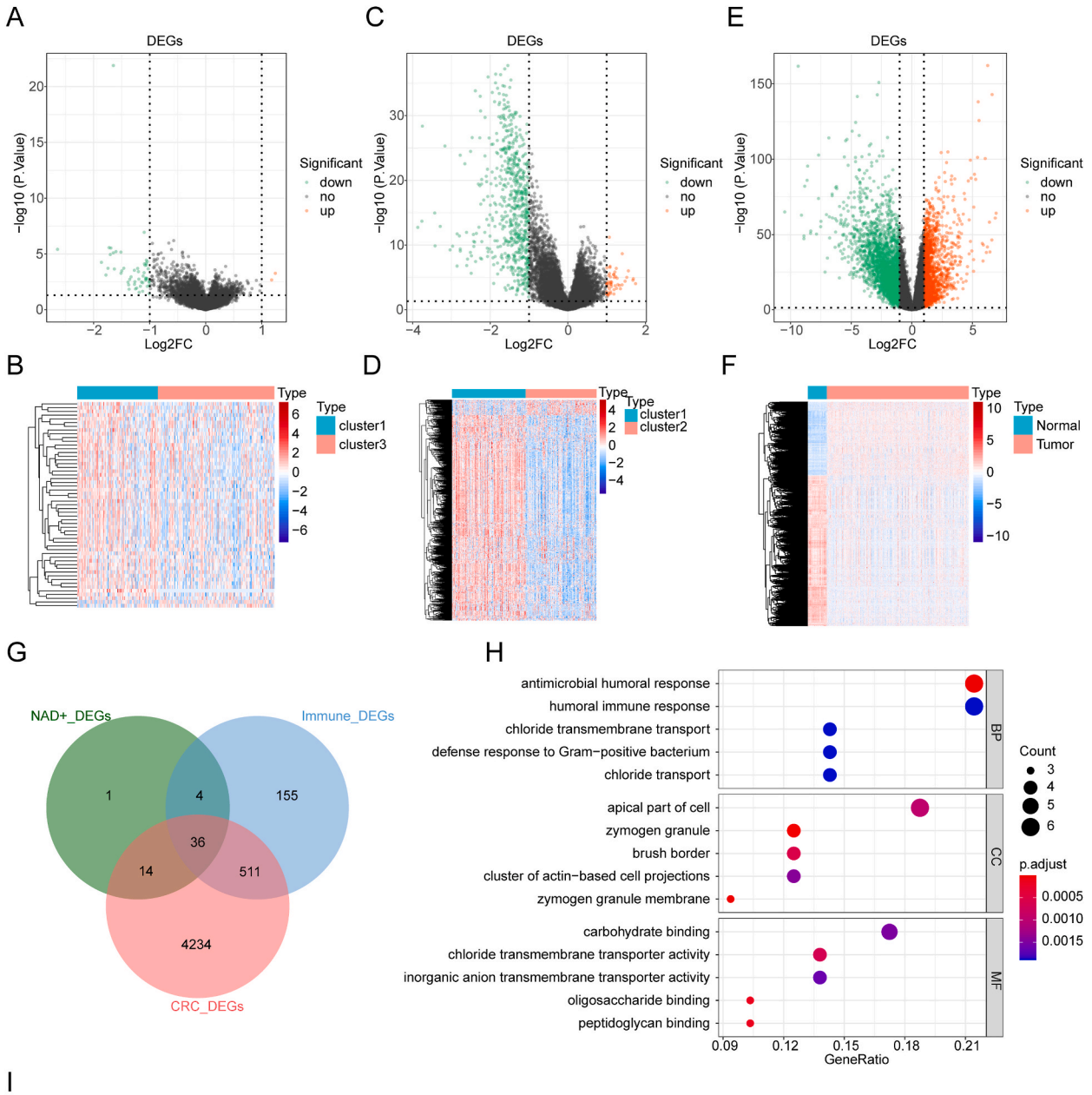

(caption on next page)

Fig. 2. Identification of differentially expressed genes (DEGs) related to NAD + metabolism and immune responses (A) Volcano plot of DEGs between NAD + metabolism-related cluster 3 and cluster 1. (B) Heatmap of DEGs between NAD + metabolism-related cluster 3 and cluster 1. (C) Volcano plot of DEGs between immune-related cluster 2 and cluster 1. (D) Heatmap of DEGs between immune-related cluster 2 and cluster 1. (E) Volcano plot of DEGs between CRC and normal samples in The Cancer Genome Atlas-Colorectal Cancer (TCGA-CRC) dataset. (F) Heatmap of DEGs between CRC and normal samples in the TCGA-CRC dataset. (G) Candidate genes were obtained from the Venn diagram of NAD + metabolic DEGs, immune-related DEGs and CRC DEGs. (H) Gene Ontology (GO) enrichment pathway of candidate genes. (I) Kyoto Encyclopedia of Genes and Genomes (KEGG) enrichment pathway of candidate genes.

Table 2
The list of NAD + metabolism and immune-related differentially expressed genes (DEGs) in colorectal cancer (CRC).

Symbol	logFC	AveExpr	t	P.Value	adj.P.Val	B
IGJ	−3.75E+00	9.94E+00	−1.27E+01	4.30E-29	1.63E-26	5.54E+01
DNASE1L3	−2.65E+00	3.80E+00	−1.10E+01	2.77E-23	3.79E-21	4.22E+01
DMBT1	−3.43E+00	9.94E+00	−8.55E+00	1.10E-15	5.90E-14	2.50E+01
ITLN1	−3.76E+00	6.26E+00	−8.11E+00	2.06E-14	9.72E-13	2.21E+01
CLCA4	−3.29E+00	5.07E+00	−7.83E+00	1.30E-13	5.69E-12	2.03E+01
PLAC8	−1.88E+00	8.49E+00	−7.83E+00	1.30E-13	5.70E-12	2.03E+01
CLCA1	−3.87E+00	7.65E+00	−7.78E+00	1.83E-13	7.88E-12	2.00E+01
FCGBP	−2.61E+00	1.18E+01	−7.50E+00	1.08E-12	4.29E-11	1.82E+01
MUC4	−2.36E+00	9.27E+00	−7.43E+00	1.59E-12	6.18E-11	1.79E+01
PLA2G2A	−2.85E+00	9.29E+00	−7.41E+00	1.85E-12	7.13E-11	1.77E+01
B3GNT6	−2.79E+00	4.87E+00	−7.29E+00	3.88E-12	1.44E-10	1.70E+01
HEPACAM2	−2.40E+00	5.81E+00	−6.93E+00	3.45E-11	1.09E-09	1.48E+01
DUOXA2	−2.42E+00	7.54E+00	−6.66E+00	1.62E-10	4.75E-09	1.33E+01
DHRS9	−2.07E+00	6.38E+00	−6.56E+00	3.02E-10	8.46E-09	1.27E+01
SPINK4	−2.77E+00	7.41E+00	−6.51E+00	4.00E-10	1.10E-08	1.25E+01
MUC2	−3.03E+00	1.11E+01	−6.45E+00	5.55E-10	1.50E-08	1.21E+01
ZG16	−2.77E+00	5.45E+00	−6.38E+00	8.23E-10	2.17E-08	1.18E+01
SLC6A14	−2.05E+00	6.83E+00	−6.34E+00	1.04E-09	2.71E-08	1.15E+01
BEST2	−1.96E+00	3.01E+00	−6.31E+00	1.22E-09	3.14E-08	1.14E+01
CA4	−2.51E+00	4.44E+00	−6.29E+00	1.35E-09	3.45E-08	1.13E+01
CA1	−2.48E+00	3.34E+00	−6.07E+00	4.49E-09	1.05E-07	1.01E+01
FAM55A	−2.07E+00	6.46E+00	−6.03E+00	5.69E-09	1.32E-07	9.88E+00
C6orf105	−1.72E+00	6.49E+00	−6.00E+00	6.64E-09	1.52E-07	9.73E+00
SI	−2.25E+00	5.09E+00	−5.92E+00	1.03E-08	2.25E-07	9.31E+00
MS4A12	−2.22E+00	4.04E+00	−5.86E+00	1.43E-08	3.04E-07	8.99E+00
PIGR	−2.58E+00	1.38E+01	−5.86E+00	1.44E-08	3.06E-07	8.98E+00
CEACAM7	−1.91E+00	9.83E+00	−5.47E+00	1.06E-07	1.85E-06	7.05E+00
REG1B	−2.61E+00	4.79E+00	−5.41E+00	1.43E-07	2.44E-06	6.76E+00
REG1A	−2.85E+00	8.18E+00	−5.38E+00	1.71E-07	2.89E-06	6.59E+00
B4GALNT2	−1.72E+00	2.99E+00	−5.11E+00	6.37E-07	9.42E-06	5.32E+00
CHGA	−1.81E+00	4.13E+00	−4.78E+00	2.90E-06	3.58E-05	3.87E+00
MOGAT2	−1.19E+00	5.53E+00	−4.30E+00	2.39E-05	2.26E-04	1.86E+00
VSIG2	−1.43E+00	6.73E+00	−3.61E+00	3.67E-04	2.27E-03	−7.18E-01
SLC26A3	−1.49E+00	9.28E+00	−3.51E+00	5.34E-04	3.09E-03	−1.07E+00
FAM55D	−1.30E+00	7.02E+00	−3.24E+00	1.36E-03	6.69E-03	−1.93E+00
COMP	1.19E+00	5.63E+00	3.40E+00	7.84E-04	4.24E-03	−1.43E+00

Consequently, *MOGAT2*, *DNASE1L3*, and *COMP* were selected as the three optimal NAD + metabolism-immune-relevant prognostic genes for establishing a prognostic signature. Subsequently, we derived a prognostic signature using the following formula: RiskScore $=$ (-0.05458234) $\times$ expression (MOGAT2) + (-0.08772365) $\times$ expression.

(DNASE1L3) + 0.05830732 $\times$ expression (COMP). Using this formula, we computed the risk score for each CRC patient in the training set and classified them into two risk subgroups (high-risk and low-risk) using the optimal cutoff value (Fig. 3D). Principal component analysis (PCA) revealed a clear distinction between the high- and low-risk groups based on the expression of the three prognostic genes (Supplementary Fig. 1A). The Kaplan–Meier curve demonstrated that patients at greater risk had significantly poorer survival than those at lower risk (Fig. 3E). ROC curves were plotted to assess the predictive efficiency of the signature. The area under the curve (AUC) values for OS in the training set were all greater than 0.6 (1-, 3-, and 5-year), indicating decent accuracy (Fig. 3F). Fig. 3D displays the distribution of the ranked risk score and survival status for each patient in the training set. Survival status revealed that as the risk score increased, patients had a relatively greater risk of death. The expression heatmap showed that *COMP* was highly expressed in patients with higher risk scores, whereas *DNASE1L3* and *MOGAT2* were highly expressed in patients with lower risk scores (Fig. 3D). To further validate the applicability and reliability of the risk signature, the above analysis was also conducted in the testing set and external validation set (GSE17538). A consistent trend was observed in the testing set and external validation set (Fig. 3G-L, Supplementary Fig. 1B-C. These results indicate that the NAD + metabolism-immune-related prognostic signature serves as a valid survival predictor for CRC patients.

Table 3
The Gene Ontology (GO) enrichment results of NAD + metabolism- and immune-related DEGs.

ONTOLOGY	ID	Description	GeneRatio	BgRatio	pvalue	p. adjust	qvalue	geneID
BP	GO:0019730	antimicrobial humoral response	6/28	142/18862	5.38E-08	2.64E-05	2.05E-05	CHGA/ITLN1/REG1A/PLA2G2A/REG1B/DMBT1
BP	GO:1902476	chloride transmembrane transport	4/28	96/18862	1.17E-05	1.90E-03	1.48E-03	CLCA4/BEST2/SLC26A3/CLCA1
BP	GO:0050830	defense response to Gram-positive bacterium	4/28	98/18862	1.27E-05	1.90E-03	1.48E-03	CHGA/ZG16/PLA2G2A/DMBT1
BP	GO:0006959	humoral immune response	6/28	380/18862	1.66E-05	1.90E-03	1.48E-03	CHGA/ITLN1/REG1A/PLA2G2A/REG1B/DMBT1
BP	GO:0006821	chloride transport	4/28	109/18862	1.94E-05	1.90E-03	1.48E-03	CLCA4/BEST2/SLC26A3/CLCA1
BP	GO:0098661	inorganic anion transmembrane transport	4/28	120/18862	2.83E-05	2.31E-03	1.80E-03	CLCA4/BEST2/SLC26A3/CLCA1
BP	GO:0015701	bicarbonate transport	3/28	43/18862	3.47E-05	2.43E-03	1.89E-03	CA1/CA4/SLC26A3
BP	GO:0007586	digestion	4/28	138/18862	4.90E-05	3.00E-03	2.33E-03	MOGAT2/SI/MUC4/MUC2
BP	GO:0016266	O-glycan processing	3/28	61/18862	9.95E-05	5.42E-03	4.20E-03	B3GNT6/MUC4/MUC2
BP	GO:0015698	inorganic anion transport	4/28	171/18862	1.13E-04	5.52E-03	4.28E-03	CLCA4/BEST2/SLC26A3/CLCA1
BP	GO:0042742	defense response to bacterium	5/28	344/18862	1.36E-04	6.08E-03	4.71E-03	CHGA/ZG16/PLAC8/PLA2G2A/DMBT1
BP	GO:0015711	organic anion transport	5/28	376/18862	2.06E-04	8.43E-03	6.54E-03	CA1/CA4/SLC26A3/SLC6A14/PLA2G2A
BP	GO:0022600	digestive system process	3/28	99/18862	4.18E-04	1.43E-02	1.11E-02	MOGAT2/MUC4/MUC2
BP	GO:0006486	protein glycosylation	4/28	250/18862	4.80E-04	1.43E-02	1.11E-02	B4GALNT2/B3GNT6/MUC4/MUC2
BP	GO:0043413	macromolecule glycosylation	4/28	250/18862	4.80E-04	1.43E-02	1.11E-02	B4GALNT2/B3GNT6/MUC4/MUC2
BP	GO:0030277	maintenance of gastrointestinal epithelium	2/28	22/18862	4.82E-04	1.43E-02	1.11E-02	MUC4/MUC2
BP	GO:0006493	protein O-linked glycosylation	3/28	105/18862	4.96E-04	1.43E-02	1.11E-02	B3GNT6/MUC4/MUC2
BP	GO:0070085	glycosylation	4/28	263/18862	5.81E-04	1.58E-02	1.23E-02	B4GALNT2/B3GNT6/MUC4/MUC2
BP	GO:0010669	epithelial structure maintenance	2/28	29/18862	8.42E-04	2.17E-02	1.68E-02	MUC4/MUC2
BP	GO:0006730	one-carbon metabolic process	2/28	40/18862	1.60E-03	3.79E-02	2.94E-02	CA1/CA4
BP	GO:0009101	glycoprotein biosynthetic process	4/28	347/18862	1.63E-03	3.79E-02	2.94E-02	B4GALNT2/B3GNT6/MUC4/MUC2
CC	GO:0042588	zymogen granule	4/32	13/19520	4.21E-09	3.28E-07	2.44E-07	ZG16/CLCA1/REG1A/DMBT1
CC	GO:0042589	zymogen granule membrane	3/32	10/19520	4.76E-07	1.86E-05	1.38E-05	ZG16/CLCA1/DMBT1
CC	GO:0005903	brush border	4/32	101/19520	2.17E-05	5.65E-04	4.19E-04	CA4/SLC26A3/SI/ITLN1
CC	GO:0045177	apical part of cell	6/32	414/19520	4.98E-05	9.72E-04	7.21E-04	CA4/CLCA4/SLC26A3/CEACAM7/SI/DUOXA2
CC	GO:0098862	cluster of actin-based cell projections	4/32	156/19520	1.19E-04	1.43E-03	1.06E-03	CA4/SLC26A3/SI/ITLN1
CC	GO:0031526	brush border membrane	3/32	59/19520	1.22E-04	1.43E-03	1.06E-03	CA4/SLC26A3/ITLN1
CC	GO:0030667	secretory granule membrane	5/32	305/19520	1.28E-04	1.43E-03	1.06E-03	CA4/ZG16/CLCA1/PIGR/DMBT1
CC	GO:0016324	apical plasma membrane	5/32	351/19520	2.47E-04	2.41E-03	1.79E-03	CA4/CLCA4/SLC26A3/CEACAM7/SI
CC	GO:0005796	Golgi lumen	3/32	102/19520	6.15E-04	5.33E-03	3.96E-03	ZG16/MUC4/MUC2
CC	GO:0031253	cell projection membrane	4/32	337/19520	2.14E-03	1.67E-02	1.24E-02	CA4/SLC26A3/ITLN1/REG1A

(*continued on next page*)

Table 3 (*continued*)

ONTOLOGY	ID	Description	GeneRatio	BgRatio	pvalue	p. adjust	qvalue	geneID
CC	GO:0031225	anchored component of membrane	3/32	170/19520	2.67E-03	1.90E-02	1.41E-02	CA4/CEACAM7/ITLN1
MF	GO:0070492	oligosaccharide binding	3/29	16/18337	1.96E-06	1.53E-04	8.12E-05	ITLN1/REG1A/REG1B
MF	GO:0042834	peptidoglycan binding	3/29	18/18337	2.86E-06	1.53E-04	8.12E-05	ZG16/REG1A/REG1B
MF	GO:0015108	chloride transmembrane transporter activity	4/29	101/18337	1.85E-05	6.61E-04	3.51E-04	CLCA4/BEST2/SLC26A3/CLCA1
MF	GO:0030246	carbohydrate binding	5/29	267/18337	5.62E-05	1.50E-03	7.99E-04	ZG16/SI/ITLN1/REG1A/REG1B
MF	GO:0015103	inorganic anion transmembrane transporter activity	4/29	145/18337	7.64E-05	1.63E-03	8.68E-04	CLCA4/BEST2/SLC26A3/CLCA1
MF	GO:0005254	chloride channel activity	3/29	74/18337	2.14E-04	3.32E-03	1.76E-03	CLCA4/BEST2/CLCA1
MF	GO:0004089	carbonate dehydratase activity	2/29	14/18337	2.17E-04	3.32E-03	1.76E-03	CA1/CA4
MF	GO:0005229	intracellular calcium activated chloride channel activity	2/29	16/18337	2.86E-04	3.40E-03	1.81E-03	CLCA4/CLCA1
MF	GO:0061778	intracellular chloride channel activity	2/29	16/18337	2.86E-04	3.40E-03	1.81E-03	CLCA4/CLCA1
MF	GO:0005253	anion channel activity	3/29	86/18337	3.33E-04	3.57E-03	1.89E-03	CLCA4/BEST2/CLCA1
MF	GO:0005539	glycosaminoglycan binding	4/29	228/18337	4.33E-04	4.21E-03	2.24E-03	ZG16/COMP/REG1A/REG1B
MF	GO:0008509	anion transmembrane transporter activity	5/29	459/18337	6.95E-04	6.20E-03	3.29E-03	CLCA4/BEST2/SLC26A3/CLCA1/SLC6A14
MF	GO:0022839	ion gated channel activity	2/29	42/18337	2.00E-03	1.65E-02	8.74E-03	CLCA4/CLCA1
MF	GO:0008376	acetylgalactosaminyltransferase activity	2/29	47/18337	2.50E-03	1.91E-02	1.01E-02	B4GALNT2/B3GNT6
MF	GO:0016836	hydro-lyase activity	2/29	64/18337	4.58E-03	3.27E-02	1.74E-02	CA1/CA4
MF	GO:0016835	carbon-oxygen lyase activity	2/29	79/18337	6.90E-03	4.61E-02	2.45E-02	CA1/CA4

Table 4
The Kyoto Encyclopedia of Genes and Genomes (KEGG) enrichment results of NAD + metabolism- and immune-related DEGs.

KEGG	ID	Description	GeneRatio	BgRatio	pvalue	p.adjust	qvalue	geneID
	hsa04972	Pancreatic secretion	4.54E+04	102/8149	3.75E-05	1.13E-03	9.08E-04	22802/1811/1179/5320
	hsa00910	Nitrogen metabolism	4.53E+04	17/8149	4.83E-04	7.25E-03	5.85E-03	759/762
	hsa04975	Fat digestion and absorption	4.53E+04	43/8149	3.11E-03	3.11E-02	2.51E-02	80168/5320

3.4. Relativity analysis of clinical parameters and the NAD + metabolism-immune-relevant prognostic signature

To explore the associations between the NAD + metabolism-immune-related prognostic signature and clinical factors, we compared the risk scores of patients in different clinical subgroups. As shown in Fig. 4A-F, the NAD + metabolism-immune-related risk score was correlated with pathologic T stage, pathologic N stage, and stage (p value < 0.05) but was not correlated with age, sex, or pathologic M stage.

3.5. The nomogram containing the NAD + metabolism-immune-relevant risk score as an independent prognostic predictor

Cox analysis (univariate Cox and multivariate Cox) revealed that the risk score, pathologic T stage, and pathologic M stage were independent predictors of prognosis for CRC patients Fig. 5A-B, p value < 0.05). A nomogram incorporating these independent prognostic predictors was generated Fig. 5C). The C-index of the nomogram was 0.7582962, and calibration curves demonstrated the satisfactory performance of the nomogram in predicting survival at 1, 3, and 5 years for CRC patients (Fig. 5D).

3.6. Association of the NAD + metabolism-immune-related prognostic signature with the immune microenvironment

The GSVA algorithm demonstrated that patients in the low-risk subgroup had higher scores for immune-related pathways, such as APC coinhibition, CCR, MHC class I, and T-cell costimulation Fig. 6A). Using the ssGSEA algorithm, we calculated the fraction of each

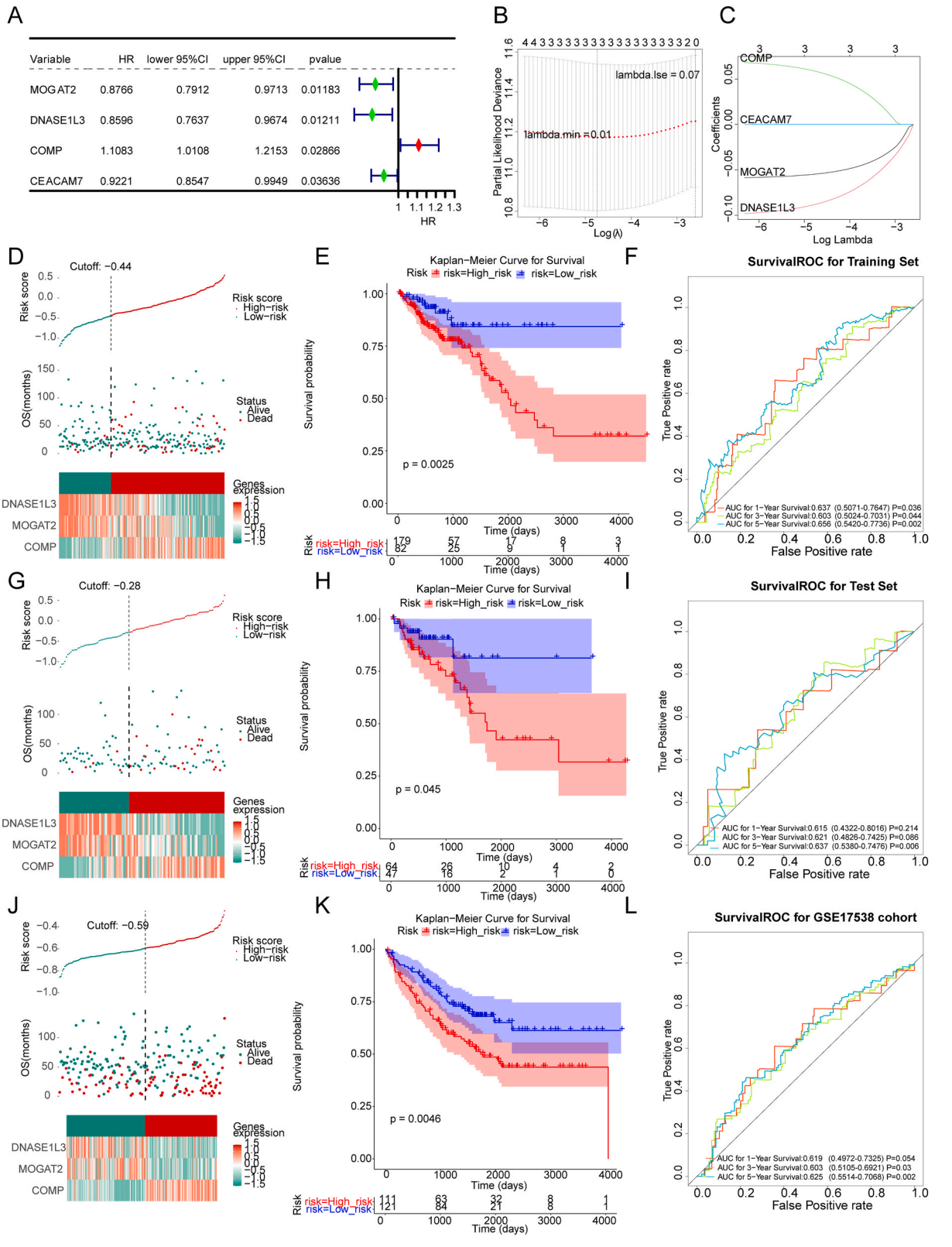

(caption on next page)

Fig. 3. The NAD + metabolism-immune-relevant prognostic signature for CRC. (A) Univariate forest plot of the correlation between prognostic gene expression and overall survival (OS) in CRC patients. (B) Deviance plot of partial likelihood determined by least absolute shrinkage and selection operator (LASSO) Cox regression analysis. (C) Graph of the gene coefficients. The abscissa is log(Lambda), and the ordinate is the coefficient corresponding to the gene. Risk curve, scatter plot, model gene expression heatmap, Kaplan–Meier (K–M) survival analysis and receiver operating characteristic (ROC) curve of patients with high or low risk in different sets. (D–F) Training set. (G–I) Test set. (J–L) External verification set.

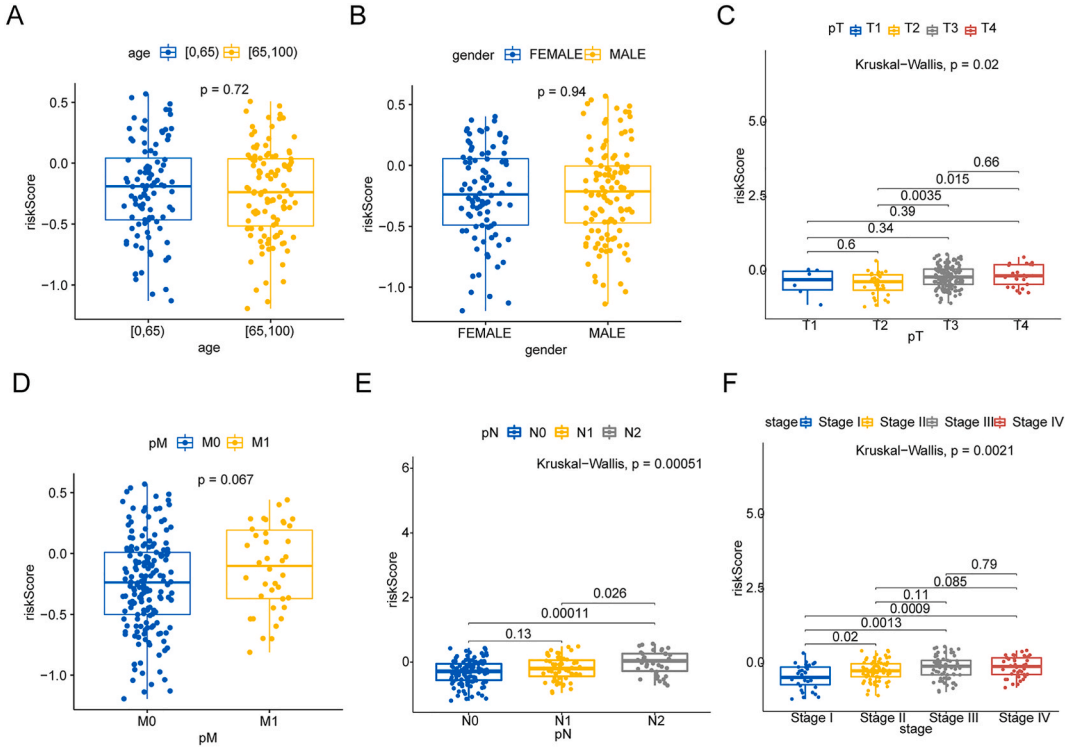

Fig. 4. Risk score analysis of different clinicopathological features. The distribution of risk scores between high- and low-risk patients was stratified according to (A) age, (B) sex, (C) pathological T stage, (D) pathological M stage, (E) pathological N stage and (F) stage.

immune infiltration cell for samples in both risk subgroups. As shown in Fig. 6B, the fractions of macrophages, neutrophils, NK cells, Tems, Tgds, and Th1 cells were increased in patients with higher risk scores, whereas the fractions of aDCs, B cells, eosinophils, T cells, and Th17 cells were increased in patients with lower risk scores. To further investigate the associations between prognostic genes and immune cells in CRC, we utilized the TIMER database Fig. 6C–E). Based on thresholds of $|cor| > 0.3$ and $p < 0.05$, we found that *COMP* was notably positively correlated with $CD4^+$ T cells and macrophages Fig. 6C), whereas *DNASE1L3* was significantly positively correlated with B cells (Fig. 6D).

3.7. Association of the NAD + metabolism-immune-related prognostic signature with therapy

The immune checkpoint molecule HAVCR2 was found to be expressed at higher levels in patients with higher risk scores Fig. 6F). According to the TIDE results, patients in the low-risk group might respond better to immunotherapy than patients in the high-risk group Fig. 6G and H). We also investigated the correlation between prognostic genes and sensitivity to chemotherapy drugs (IC_{50} values) using the 'pRRophetic' package. We observed that *COMP* was associated with multiple drugs, including bryostatin.1, camptothecin, cytarabine, dasatinib, pazopanib, and shikonin (Fig. 7).

3.8. The expression of NAD + metabolism-immune-related prognostic genes

In the TCGA-CRC dataset, *MOGAT2* and *DNASE1L3* were downregulated, whereas *COMP* showed elevated expression in CRC tissues compared to normal tissues Fig. 8A). We further confirmed these expression trends in the external validation set GSE115261 Fig. 8B). To determine the changes in the expression of prognostic genes at the protein level, we obtained immunohistochemistry images from the HPA database. Unfortunately, we did not detect immunohistochemical results for *COMP* in CRC. However, we found that the protein expression of *DNASE1L3* and *MOGAT2* was lower in CRC tissues than in normal tissues Fig. 9A and B). We also analyzed the mRNA expression of prognostic genes in human normal colonic epithelial cells (CCD814) and three human CRC cell lines

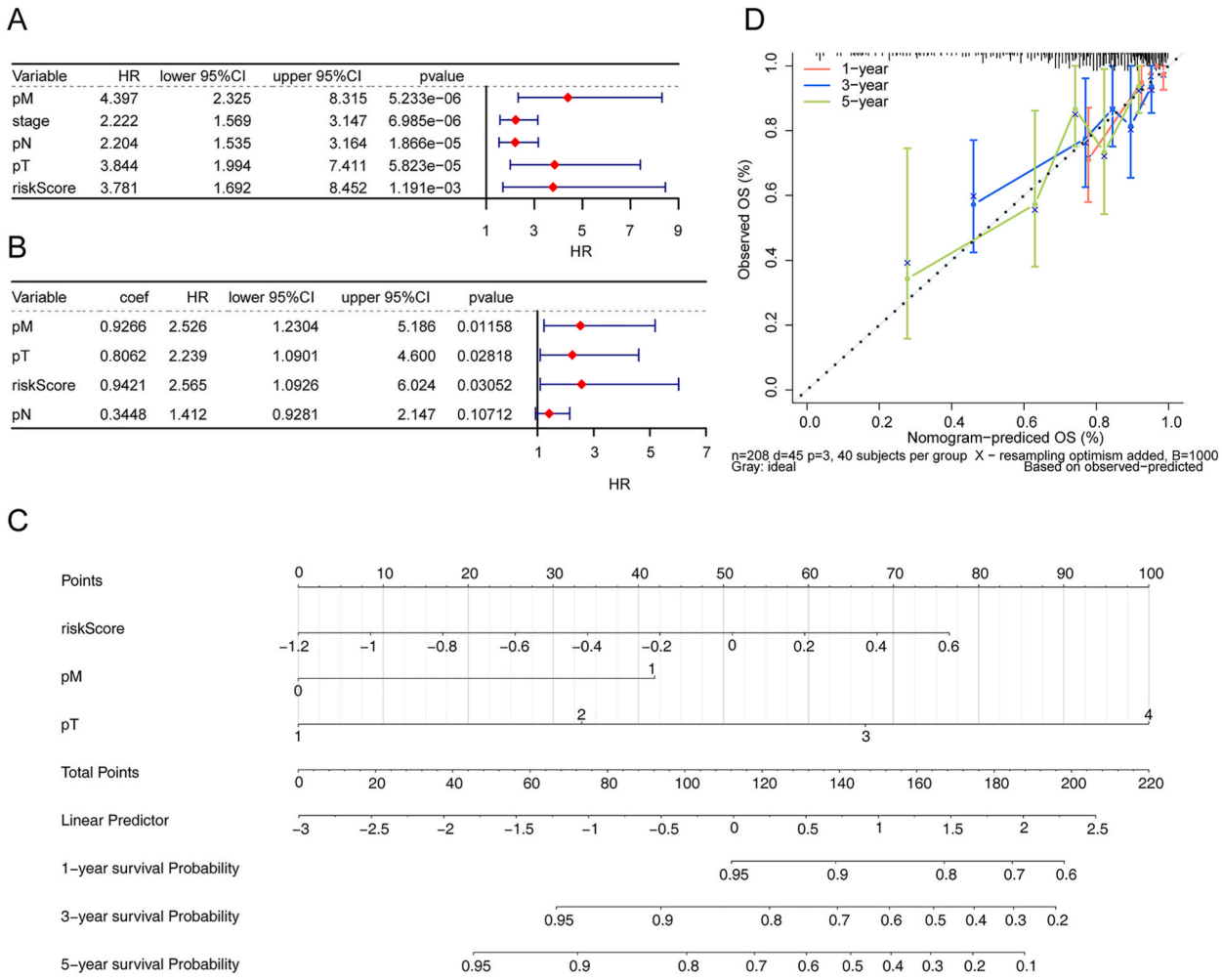

Fig. 5. TCGA-CRC independent prognosis forest map. (A) Univariate Cox analyses. The red diamond squares on the transverse lines indicate the hazard ratio (HR), and the blue transverse lines indicate the 95 % confidence interval (CI). (B) Multivariate Cox analyses. (C) Independent prognosis model nomogram. Nomograms that integrate the prediction of the probability of patient survival for 1-, 3- or 5-year OS. (D) Calibration curves of the nomogram for predicting survival outcomes at 1, 3, and 5 years. The 45-degree line represents the ideal prediction.

(HCT-116, LOVO, and SW480). Consistent with the results from public databases, *COMP* was upregulated in HCT-116, LOVO, and SW480 cells, whereas *DNASE1L3* was downregulated in LOVO and SW480 cells (Fig. 10 A-C). However, the expression of *MOGAT2* in the cell lines was inconsistent with that in the tissue samples, possibly due to the complexity of the tumor tissue.

4. Discussion

CRC is the third most prevalent malignant tumor globally, accounting for approximately one-tenth of all cancer patients, with an estimated one million new cases reported annually worldwide. It is also a prominent contributor to cancer-related deaths, accounting for 9.2 % of deaths [23]. The primary cause of death in CRC patients is the occurrence of distant metastasis. Patients without distant metastasis exhibit a 5-year survival rate of 80–90 %, whereas those with distant metastasis have a significantly lower rate of 10–20 %. During tumor cell proliferation, a substantial energy supply is needed, which mainly involves the production of mitochondrial acetyl-CoA from glucose. This raw material is then subjected to oxidation reactions via the citric acid cycle under the influence of NAD+/NADH, resulting in ATP production. These metabolic processes provide energy for tumor cell proliferation [24]. NAD + metabolism is also involved in the regulation of diverse biological functions, including immune regulation and aging [18,25]. Immune T cells have been found to be closely associated with the occurrence, development, metastasis, and invasion of tumor cells as immune recognition improves. NAD+ is capable of regulating the expression of the tumor immune checkpoint PD-L1 through epigenetic modification. This, in turn, promotes the secretion of IFNγ by T cells and facilitates tumor immune evasion. Sirt1, an NAD + metabolic enzyme, can activate cytokine secretion in antigen-presenting cells by regulating the acetylation of IRF1. Consequently, PD-L1 expression is promoted, and tumor immunity is mediated [10,26]. The immune microenvironment and immune components

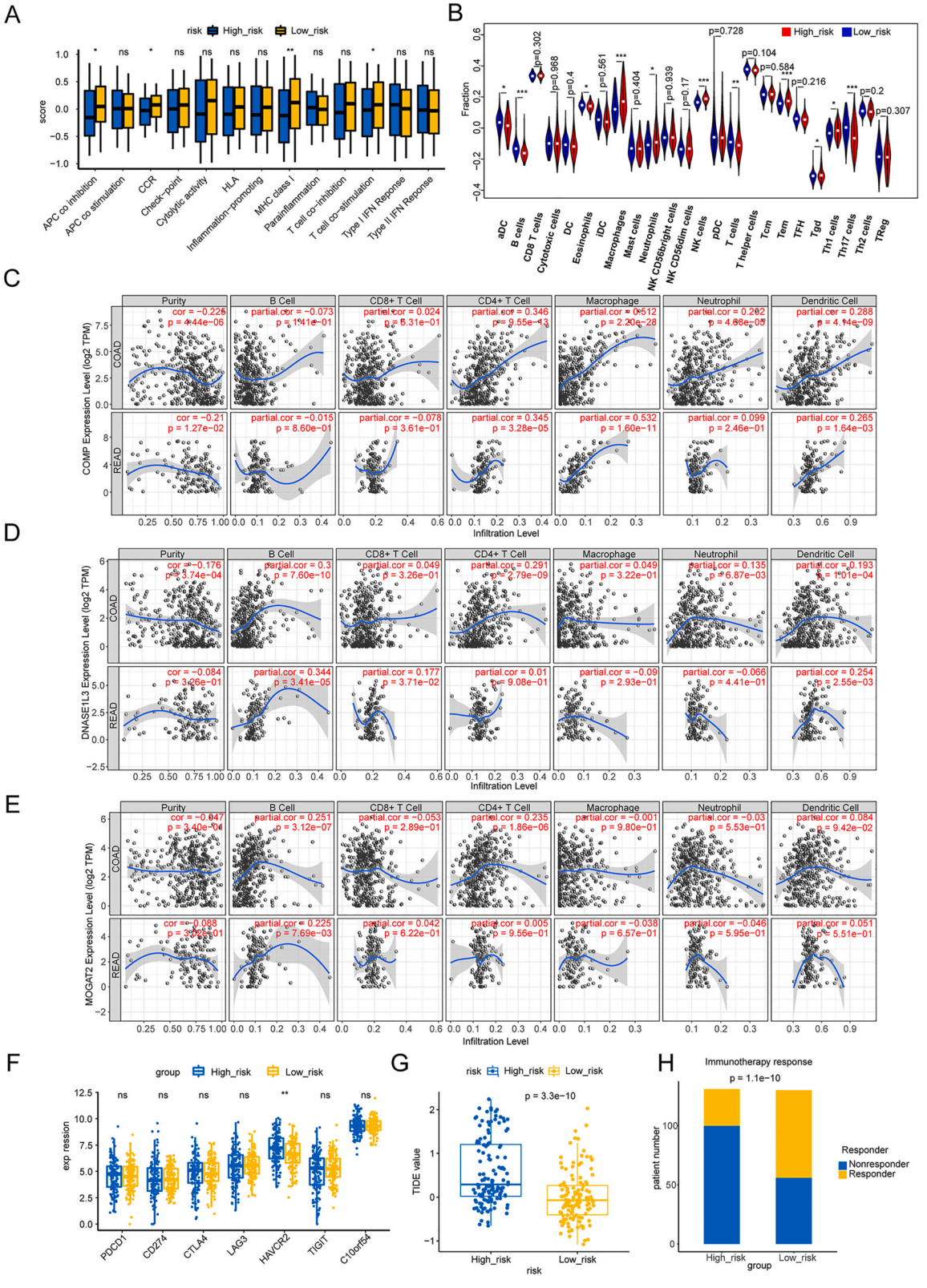

(caption on next page)

Fig. 6. Association of the NAD + metabolism-immune-related prognostic signature with the immune microenvironment. (A) Differences in 13 immune-related pathways in the high-to low-risk groups. *, $p < 0.05$; **, $p < 0.01$; ***, $p < 0.001$; ns, not significant. (B) Differences in the levels of 24 kinds of tumor-infiltrating immune cells (TIICs). (C–E) Correlations between gene expression and immune cells. The expression of COMP (C), DNASE1L3 (D), and MOGAT2 (E) correlated with that of six immune cell types. (F) Comparison of immune checkpoint expression between the high- and low-risk groups. *$p < 0.05$, **$p < 0.01$, ***$p < 0.001$, ****$p < 0.0001$, ns, not significant. (G–H) Analysis of tumor immune dysfunction and exclusion (TIDE) scores in the high- and low-risk groups. (G) Comparison of the results of the rank sum test of the TIDE score. (H) Is the number of people in the high-low-expression group who responded to immunotherapy and those who did not respond. (For interpretation of the references to color in this figure legend, the reader is referred to the Web version of this article.)

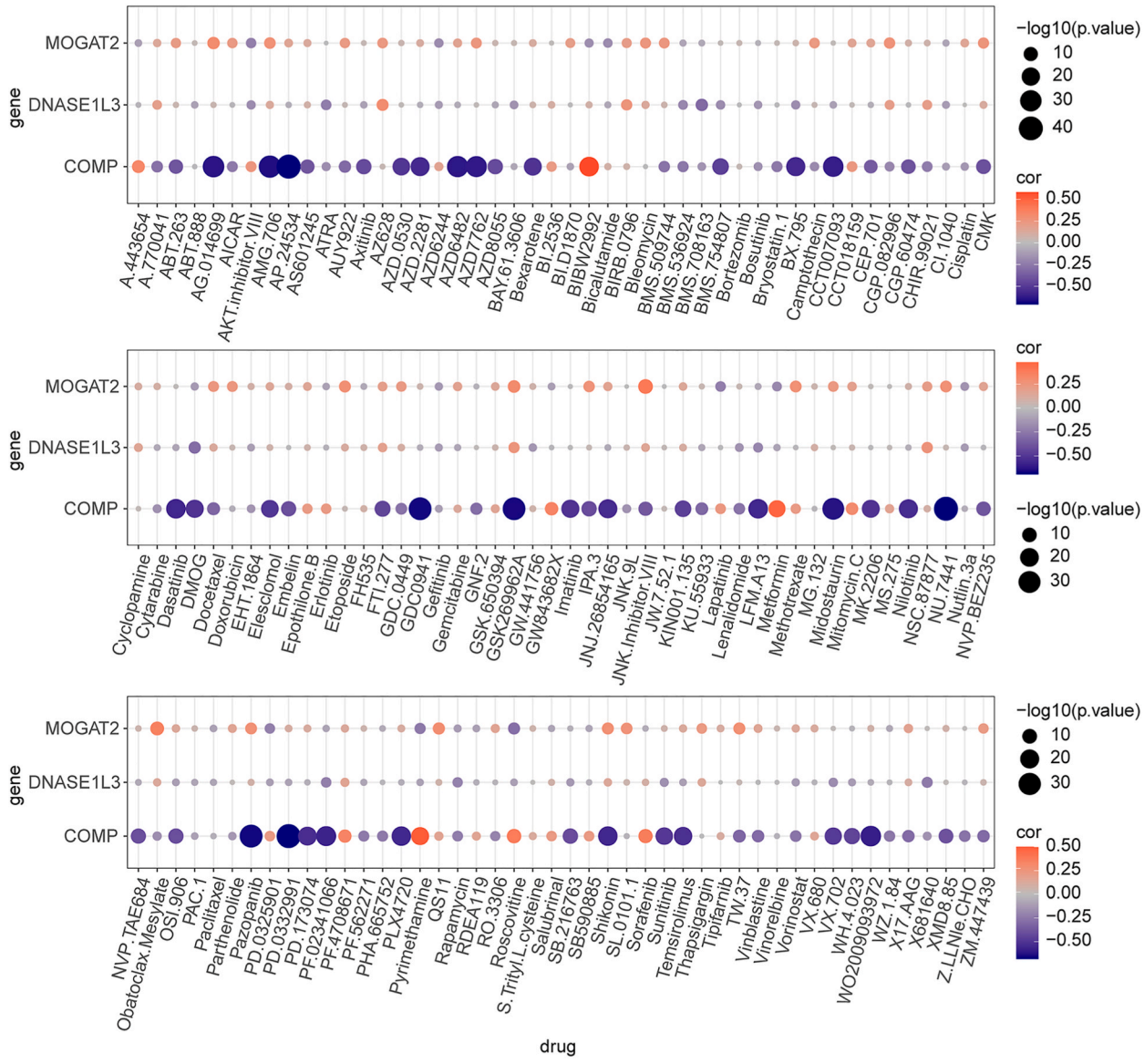

Fig. 7. Association of the NAD + metabolism-immune-related prognostic signature with therapy The red dots are positively correlated, and the blue dots are negatively correlated.

significantly impact the prognosis of cancer patients during the adaptive response to antitumor therapy [27]. However, the precise mechanisms through which NAD + metabolism regulates immune function in CRC remain unclear. Hence, we established a robust prognostic model for CRC based on NAD + metabolism and immune-related genes. This was accomplished through thorough bioinformatics analysis, immune checkpoint analysis, immune therapy response prediction, immune infiltration analysis, chemotherapy drug sensitivity analysis, and qRT−PCR validation. Our objective was to investigate the mechanisms underlying the association between NAD + metabolism and immune function in CRC.

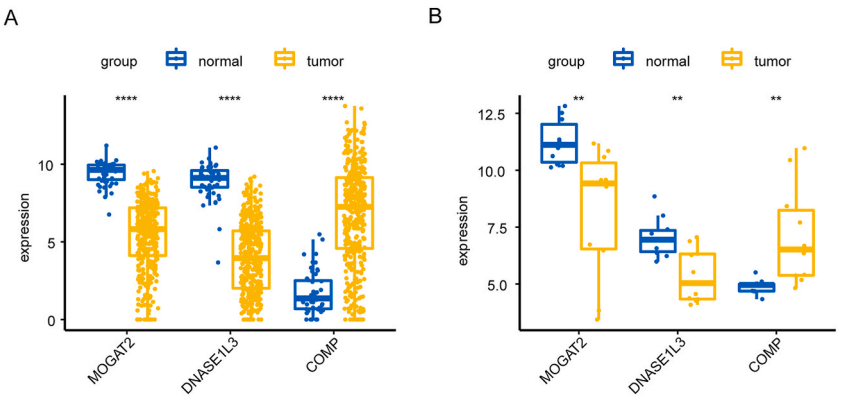

Fig. 8. Expression levels of prognostic genes in the TCGA and validation sets GSE115261. (A) TCGA-CRC. (B) GSE115261. *p < 0.05, **p < 0.01, ***p < 0.001, ****p < 0.0001. (For interpretation of the references to color in this figure legend, the reader is referred to the Web version of this article.)

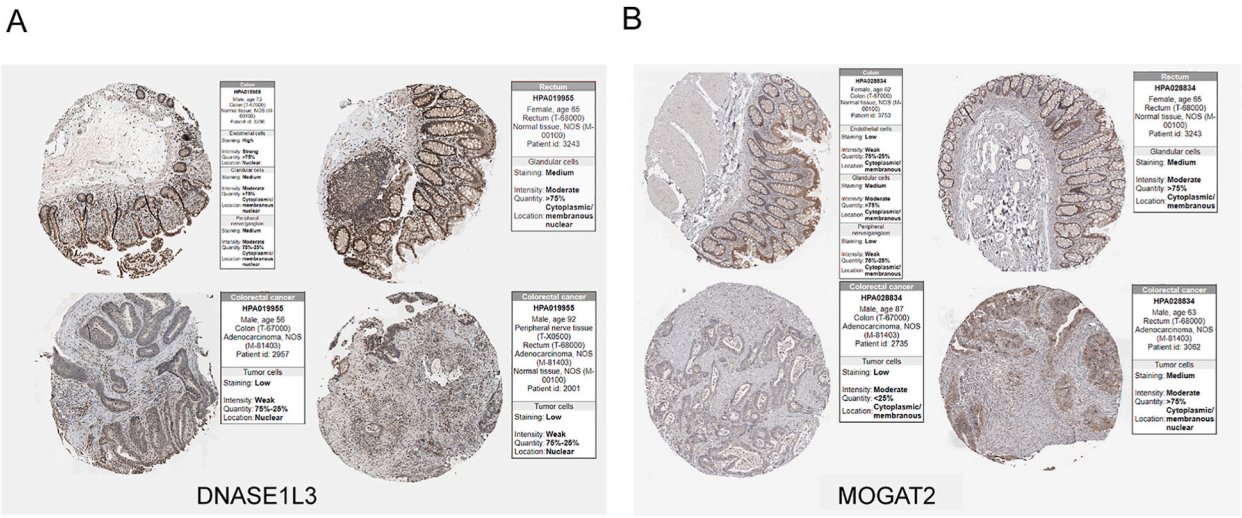

Fig. 9. Protein expression levels of prognostic characteristic genes in the Human Protein Atlas (HPA) database. (A) DNASE1L3. (B) MOGAT2.

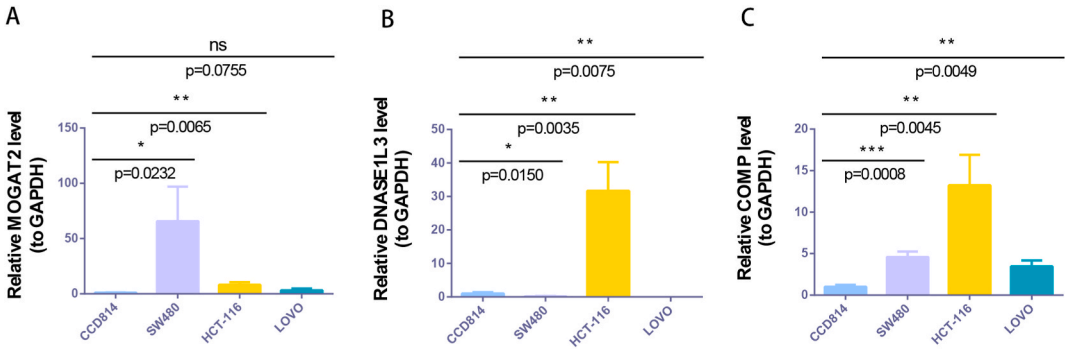

Fig. 10. mRNA expression levels of NAD + metabolic immune-related prognostic genes in CCD814, HCT-116, LOVO and SW480 cells. (A) MOGAT2. (B) DNASE1L3. (C) COMP. *p < 0.05, **p < 0.01, ***p < 0.001, ****p < 0.0001, ns, not significant.

First, a total of 36 DEGs related to NAD + metabolism and immunity were identified in CRC through differential expression analysis. These DEGs included CA1, MS4A12, CA4, CHGA, and CLCA4, among others. In CRC, the downregulation of CA1 and upregulation of ANXA4 promote the accumulation of ANXA4 on the cell membrane. Furthermore, CA1 expression is associated with

the malignant proliferation, development, differentiation, and metastasis of cancer cells [28,29]. MS4A12 is a specific storage-operated calcium channel (SOC) in the colon that facilitates Ca^{2+} influx through epidermal growth factor (EGF). This promotes chloride nitrogen metabolism, cell proliferation, and cell motility but significantly impairs chemotactic invasion [30,31]. The CLCA4 protein is expressed in secretory epithelial cells of the small intestine and affects chloride ion transmission, cell apoptosis, cell cycle control, and tumor metastasis [32].

Three genes related to NAD + metabolism and immunity were subsequently identified as prognostic genes. This was determined through univariate Cox and LASSO regression analyses. The identified genes were *MOGAT2*, *DNASE1L3*, and *COMP*. *MOGAT2* is a gene involved in fatty acid synthesis and is predominantly expressed in the human small intestine, liver, and white fat. It serves as a key rate-limiting enzyme for triglyceride synthesis in the small intestine. A study by Valerie [5] demonstrated that increased expression of adipogenic genes, including *MOGAT2*, promotes adipogenesis, proliferation, and the inflammatory response in hepatocellular carcinoma (HCC) mice, leading to liver proliferation and steatosis. Additionally, *MOGAT2* has been identified as a gene with double methylation in inflammatory breast cancer [33]. This study provides the first evidence that *MOGAT2* is a relevant prognostic gene in CRC.

Recombinant deoxyribonuclease I-like protein 3 (*DNASE1L3*) is a highly expressed secreted enzyme that plays a crucial role in regulating DNA and chromatin autoimmunity. It has been observed that *DNASE1L3* can degrade the extracellular chromatin of apoptotic bodies. Studies have shown that mutations in *DNASE1L3* are closely associated with the phenotype of lupus [34]. Moreover, there is evidence linking *DNASE1L3* deficiency to inflammatory bowel disease [34].

Recent research has suggested that *DNASE1L3* is involved in cell apoptosis, proliferation, invasion, and metastasis. It has emerged as a potential prognostic biomarker in lung adenocarcinoma and colon cancer studies, although its specific mechanism of action remains unclear [35,36]. Notably, Han's study [37] highlighted the regulatory effect of *DNASE1L3* in HCC. *DNASE1L3* is expressed in the endoplasmic reticulum, and it is secreted from the cell. Following apoptosis induction, its endoplasmic reticulum-targeted gene sequence is cleaved and translocated to the nucleus. *DNASE1L3* also acts as a plasma nuclease in the digestive cycle, aiding in the evasion of phagocytosis after apoptosis.

In the context of HCC, Li [38] discovered that *DNASE1L3* negatively regulates disease. By binding to β-chain proteins, *DNASE1L3* inhibits their nuclear translocation, thereby restraining the proliferation and metastasis of HCC cells. Mechanistically, *DNASE1L3* promotes β-ubiquitination-related degradation of catenin and disrupts the recruitment of the β-catenin disruption complex. Consequently, downstream targets such as c-Myc, P21, and P27 are inhibited, effectively controlling the cell cycle and EMT signaling. Research by SUN [39] further supports these findings by demonstrating that *DNASE1L3* significantly reduces HCC cell proliferation, colony formation, migration, and invasion in vitro. It also inhibited the formation of subcutaneous tumors in nude mice in vivo. In a mouse model, overexpression of *DNASE1L3* inhibited AKT/NRASV12-induced liver cancer, whereas *DNASE1L3* deficiency exacerbated DEN/CCl-induced liver cancer in *DNASE1L3* mice. Systemic analysis revealed that *DNASE1L3* impairs HCC cell cycle progression by interacting with CDK2 and inhibiting CDK2-stimulated E2F1 activity. C-terminal deletion of *DNASE1L3* reduces its interaction with CDK2 and eliminates its inhibitory effect on HCC.

Furthermore, Li [40] established a mouse model of colon cancer and demonstrated that the absence of *DNASE1L3* in the tumor microenvironment is associated with tumor occurrence and development. Additionally, it enhances antitumor immunity.

Cartilage oligomeric matrix protein (*COMP*) is an extracellular matrix protein that plays a crucial role in cellular phenotype regulation during histogenesis and remodeling. Recent research has focused on investigating the involvement of *COMP* in various diseases, such as liver fibrosis and pulmonary fibrosis [41,42]. In the context of colon cancer-related diseases, experimental studies have confirmed that the overexpression of *COMP* is associated with the carcinogenic effects of colon cancer, as well as with the infiltration of CAFs and M2 macrophages [43]. In liver malignancies, Li [44] discovered that the *COMP*/CD36 signaling pathway leads to the phosphorylation of ERK and AKT, resulting in the upregulation of markers associated with EMT, including MMP-2/9, Slug, and Twist, in HCC cells. This, in turn, influences tumor development. Furthermore, Blom's research [45] revealed a positive correlation between *COMP* expression and TNM stage and tumor differentiation. Additionally, a negative correlation has been identified between *COMP* expression and the presence of PD-L1 on tumor cells and immune cells. Tumor fibrosis is associated with high levels of *COMP* expression in the extracellular matrix, and tumors with dense fibrosis and elevated *COMP* expression exhibit less infiltration of immune cells. Moreover, Dakhova [46] demonstrated that knockdown of the *COMP* gene affects the expression of genes associated with the reactive matrix in prostate stromal cell lines, leading to a decrease in tumor cell development. Our study indicated that CRC patients with elevated *COMP* expression have significantly shorter OS than those with low *COMP* expression. Furthermore, we observed reduced T-cell infiltration in tumors with high *COMP* expression. Notably, we also conducted qRT−PCR experiments to validate the expression of *MOGAT2*, *DNASE1L3*, and *COMP* in CRC cells, confirming their significant difference in expression between human colon cancer cells (HCT116 and SW480) and normal colon epithelial cells (CCD814). However, no difference was observed in LOVO cells. These findings suggest that *MOGAT2*, *DNASE1L3*, and *COMP* may play a role in cell apoptosis, proliferation, invasion, and metastasis in CRC, providing potential clinical prognostic markers for this disease.

In addition, we observed significant differences in 11 types of immune cells (aDCs, B cells, eosinophils, macrophages, neutrophils, NK cells, T cells, Tem cells, Tgd cells, Th1 cells, and Th17 cells) between the CRC and control groups. We also identified four immune pathways (APC coinhibition, CCR, MHC class I, and T-cell costimulation pathways) that exhibited significant differences. Hence, it is reasonable to speculate that *MOGAT2*, *DNASE1L3*, and *COMP* may exert their effects on these 11 immune cells through the four immune signaling pathways mentioned above, ultimately regulating cell apoptosis, proliferation, invasion, and metastasis in CRC.

By comparing the rank sum test results of TIDE scores, we obtained correlations between *MOGAT2*, *DNASE1L3*, and *COMP* model genes and IC_{50}. Among them, we found that the correlations between *COMP* and AG.014699, AMG.706, AP.24534, AZD6482, AZD7762, CCT007093, GDC0941, GSK26962A, midostaurin, NU.7441, pazopanib, and PD.0332991 were less than −0.6, indicating a

significant strong negative correlation. Based on the results of the immunotherapy and chemotherapy sensitivity analyses, *MOGAT2*, *DNASE1L3*, and *COMP* inhibited the occurrence and development of CRC. Therefore, these three prognostic genes play a crucial role in the clinical treatment of patients. Interfering with *MOGAT2*, *DNASE1L3*, and *COMP* can regulate the development of tumors and improve patient quality of life. Additionally, this study provides new insights for the development of *COMP*-related chemotherapy drugs for the clinical treatment of CRC.

This study has several notable advantages. First, we employed various analytical methods, including differential gene expression analysis, enrichment analysis, Cox analysis, and the LASSO algorithm, and validated the results using multiple datasets to ensure accuracy and reliability. Second, we established and clinically validated a prognostic model, highlighting the significance and effectiveness of the model genes in determining CRC prognosis. Finally, by analyzing immune cells and pathways, we revealed immune mechanisms relevant to CRC prognosis, offering new perspectives for personalized treatment. Overall, this study excelled in methodology, results, and clinical applications, providing valuable implications for the treatment and prognosis improvement of CRC patients. However, there are several limitations to consider. First, the number of clinical samples collected in our study was limited, and future validation will require a larger sample size. Second, additional in vitro experiments were not conducted to validate the potential mechanisms of CRC identified in this study, necessitating further experimental validation of the study's findings.

5. Conclusion

In summary, this study revealed that NAD + metabolism and immune-related genes (*MOGAT2*, *DNASE1L3*, and *COMP*) are associated with CRC prognosis. Additionally, a prognostic signature based on NAD + metabolism and immune-related factors was developed for stratifying the survival risk of CRC patients. These findings provide valuable insights for future investigations on NAD + metabolism, immune-related prognostic characteristics, and the potential to minimize unnecessary steps and economic losses in experimental research. Moving forward, further exploration of the underlying mechanisms involving the three identified genes (*MOGAT2*, *DNASE1L3*, and *COMP*) in the progression of CRC is warranted. However, it is important to note that this study is retrospective and relies on public database data. To effectively apply the analysis results and prognostic models, more clinical samples and extensive data support and validation are necessary. Moreover, additional experimental research is required to fully understand the mechanisms of action of the identified genes related to NAD + metabolism and immune-related prognosis.

Ethics approval

This study was conducted in accordance with the World Medical Association Declaration of Helsinki. The data from TCGA and GEO are all accessible to the public; the current research followed the data access policies and publishing guidelines of TCGA and GEO. This study was reviewed and deemed exempt by our local ethics committee.

Consent to participate

The data was obtained through public database, which has been widely agreed, all personal information had already been anonymized to protect the individuals' privacy. For these reasons, the study protocol was exempt from the requirement to obtain informed consent from the participants.

Funding

This work was supported by (1) Guiyang Science and Technology Bureau, the First Affiliated Hospital of Guizhou University of Traditional Chinese Medicine, Great Health Science and Technology Cooperation Project (Zhuke Contract [2019] 9-2-8); (2) Research Project of Traditional Chinese Medicine and Ethnic Medicine Science and Technology of Guizhou Provincial Administration of Traditional Chinese Medicine (No. QZYY-2019-18); (3) National Natural Science Foundation of China Post-subsidy Funds for Scientific Research and Innovation Exploration Special Project (No. 2019YFC171250403); (4) Scientific Research Start-up Fund Project of Guizhou University of Traditional Chinese Medicine (GuiZhongYiKeYuanNei No. [2019]19); (5) Doctoral Startup Fund of the First Affiliated Hospital of Guizhou University of Traditional Chinese Medicine (No. GYZYYFY-BS-2018(10) and No. GYZYYFY-BS-2019 (03)); (6) National Innovation and Entrepreneurship Training Program for College Students (GuiZhongYiDaChuangHeZi (2022) No.1).

Data availability statement

The datasets used in this study were available in online repositories. Here were the URLs for the databases used in this research. The datasets used and analyzed in the current study are available from the UCSC database (https://xenabrowser.net), GEO database (https://www.ncbi.nlm.nih.gov/gds), KEGG database (https://www.genome.jp/kegg/pathway.html), Reactome database (https://reactome.org/) and ImmPort database (https://immport.niaid.nih.gov), TIMER database (https://cistrome.shinyapps.io/timer/), Jvenn website (http://jvenn.toulouse.inra.fr/app/example.html).

CRediT authorship contribution statement

Tao Ye: Writing – review & editing, Writing – original draft, Resources, Funding acquisition, Data curation, Conceptualization.

Hong Huang: Writing – review & editing, Writing – original draft, Data curation, Conceptualization. **Kangli Chen:** Software, Methodology. **Yuanao Yu:** Software, Methodology. **Dongqin Yue:** Validation. **Li Jiang:** Validation. **Huixian Wu:** Validation. **Ning Zhang:** Visualization, Supervision, Resources, Project administration, Methodology, Funding acquisition.

Declaration of competing interest

The authors declare that they have no known competing financial interests or personal relationships that could have appeared to influence the work reported in this paper.

Acknowledgments

All authors would like to thank the reviewers for their helpful comments on this paper.

Abbreviations

CRC	colorectal cancer
NAD+	nicotinamide adenine dinucleotide
LASSO	least absolute shrinkage and selection operator
GSVA	gene set variation analysis
ssGSEA	single sample gene set enrichment analysis
TIDE	tumor immune dysfunction and exclusion
HPA	Human Protein Atlas
TCGA-CRC	The Cancer Genome Atlas-Colorectal Cancer
GEO	Gene Expression Omnibus
NMRGs	NAD + metabolism-related genes
KEGG	Kyoto Encyclopedia of Genes and Genomes
IRGs	immune-related genes
DEGs	differentially expressed genes
GO	Gene Ontology
CC	cellular component
MF	molecular function
BP	biological process
ROC	receiver operating characteristic
K−M	Kaplan−Meier
ICI	immune checkpoint inhibitor
IC_{50}	half maximal inhibitory concentration
OS	overall survival
HR	hazard ratio
AUC	area under curve
PCA	principal component analysis
SOCs	storage-operated calcium channels
EGF	epidermal growth factor
MOGAT2	monoacylglycerol O-acyltransferase 2
HCC	hepatocellular carcinoma
DNASE1L3	deoxyribonuclease I-like protein 3
COMP	cartilage oligomeric matrix protein
CI	confidence interval
CDF	cumulative distribution function
SE	standard.

Appendix A. Supplementary data

Supplementary data to this article can be found online at https://doi.org/10.1016/j.heliyon.2024.e34403.

References

[1] H. Sung, J. Ferlay, R.L. Siegel, M. Laversanne, I. Soerjomataram, A. Jemal, F. Bray, Global cancer statistics 2020: GLOBOCAN estimates of incidence and mortality worldwide for 36 cancers in 185 countries, CA Cancer J Clin 71 (3) (2021) 209–249, https://doi.org/10.3322/caac.21660.

[2] M. Fleming, S. Ravula, S.F. Tatishchev, H.L. Wang, Colorectal carcinoma: pathologic aspects, J. Gastrointest. Oncol. 3 (3) (2012) 153–173, https://doi.org/10.3978/j.issn.2078-6891.2012.03.

[3] G. Buccafusca, I. Proserpio, A.C. Tralongo, S. Rametta Giuliano, P. Tralongo, Early colorectal cancer: diagnosis, treatment and survivorship care, Crit. Rev. Oncol. Hematol. 136 (2019) 20–30, https://doi.org/10.1016/j.critrevonc.2019.01.023.

[4] A. Sveen, S. Kopetz, R.A. Lothe, Biomarker-guided therapy for colorectal cancer: strength in complexity, Nat. Rev. Clin. Oncol. 17 (1) (2020) 11–32, https://doi.org/10.1038/s41571-019-0241-1.

[5] V. Blanc, J.D. Riordan, S. Soleymanjahi, J.H. Nadeau, I. Nalbantoglu, Y. Xie, E.A. Molitor, B.B. Madison, E.M. Brunt, J.C. Mills, D.C. Rubin, I.O. Ng, Y. Ha, L. R. Roberts, N.O. Davidson, Apobec1 complementation factor overexpression promotes hepatic steatosis, fibrosis, and hepatocellular cancer, J. Clin. Invest. 131 (1) (2021), https://doi.org/10.1172/jci138699.

[6] A.J. Covarrubias, R. Perrone, A. Grozio, E. Verdin, NAD(+) metabolism and its roles in cellular processes during ageing, Nat. Rev. Mol. Cell Biol. 22 (2) (2021) 119–141, https://doi.org/10.1038/s41580-020-00313-x.

[7] X. Liu, Y. Liu, Z. Liu, C. Lin, F. Meng, L. Xu, X. Zhang, C. Zhang, P. Zhang, S. Gong, N. Wu, Z. Ren, J. Song, Y. Zhang, CircMYH9 drives colorectal cancer growth by regulating serine metabolism and redox homeostasis in a p53-dependent manner, Mol. Cancer 20 (1) (2021) 114, https://doi.org/10.1186/s12943-021-01412-9.

[8] J.P. Murphy, M.A. Giacomantonio, J.A. Paulo, R.A. Everley, B.E. Kennedy, G.P. Pathak, D.R. Clements, Y. Kim, C. Dai, T. Sharif, S.P. Gygi, S. Gujar, The NAD(+) salvage pathway supports PHGDH-driven serine biosynthesis, Cell Rep. 24 (9) (2018), https://doi.org/10.1016/j.celrep.2018.07.086, 2381-91.e5.

[9] H. Lv, G. Lv, C. Chen, Q. Zong, G. Jiang, D. Ye, X. Cui, Y. He, W. Xiang, Q. Han, L. Tang, W. Yang, H. Wang, NAD(+) metabolism maintains inducible PD-L1 expression to drive tumor immune evasion, Cell Metabol. 33 (1) (2021), https://doi.org/10.1016/j.cmet.2020.10.021, 110-27.e5.

[10] D. Bruni, H.K. Angell, J. Galon, The immune contexture and Immunoscore in cancer prognosis and therapeutic efficacy, Nat. Rev. Cancer 20 (11) (2020) 662–680, https://doi.org/10.1038/s41568-020-0285-7.

[11] G. Jung, E. Hernández-Illán, L. Moreira, F. Balaguer, A. Goel, Epigenetics of colorectal cancer: biomarker and therapeutic potential, Nat. Rev. Gastroenterol. Hepatol. 17 (2) (2020) 111–130, https://doi.org/10.1038/s41575-019-0230-y.

[12] N.J. Llosa, M. Cruise, A. Tam, E.C. Wicks, E.M. Hechenbleikner, J.M. Taube, R.L. Blosser, H. Fan, H. Wang, B.S. Luber, M. Zhang, N. Papadopoulos, K.W. Kinzler, B. Vogelstein, C.L. Sears, R.A. Anders, D.M. Pardoll, F. Housseau, The vigorous immune microenvironment of microsatellite instable colon cancer is balanced by multiple counter-inhibitory checkpoints, Cancer Discov. 5 (1) (2015) 43–51, https://doi.org/10.1158/2159-8290.Cd-14-0863.

[13] M.D. Wilkerson, D.N. Hayes, ConsensusClusterPlus: a class discovery tool with confidence assessments and item tracking, Bioinformatics 26 (12) (2010) 1572–1573, https://doi.org/10.1093/bioinformatics/btq170.

[14] M.E. Ritchie, B. Phipson, D. Wu, Y. Hu, C.W. Law, W. Shi, G.K. Smyth, Limma powers differential expression analyses for RNA-sequencing and microarray studies, Nucleic Acids Res. 43 (7) (2015) e47, https://doi.org/10.1093/nar/gkv007.

[15] T. Wu, E. Hu, S. Xu, M. Chen, P. Guo, Z. Dai, T. Feng, L. Zhou, W. Tang, L. Zhan, X. Fu, S. Liu, X. Bo, G. Yu, clusterProfiler 4.0: a universal enrichment tool for interpreting omics data, Innovation 2 (3) (2021) 100141, https://doi.org/10.1016/j.xinn.2021.100141.

[16] S. Hänzelmann, R. Castelo, J. Guinney, GSVA: gene set variation analysis for microarray and RNA-seq data, BMC Bioinf. 14 (2013) 7, https://doi.org/10.1186/1471-2105-14-7.

[17] G. Bindea, B. Mlecnik, M. Tosolini, A. Kirilovsky, M. Waldner, A.C. Obenauf, H. Angell, T. Fredriksen, L. Lafontaine, A. Berger, P. Bruneval, W.H. Fridman, C. Becker, F. Pagès, M.R. Speicher, Z. Trajanoski, J. Galon, Spatiotemporal dynamics of intratumoral immune cells reveal the immune landscape in human cancer, Immunity 39 (4) (2013) 782–795, https://doi.org/10.1016/j.immuni.2013.10.003.

[18] A. Chiarugi, C. Dölle, R. Felici, M. Ziegler, The NAD metabolome–a key determinant of cancer cell biology, Nat. Rev. Cancer 12 (11) (2012) 741–752, https://doi.org/10.1038/nrc3340.

[19] P. Jiang, S. Gu, D. Pan, J. Fu, A. Sahu, X. Hu, Z. Li, N. Traugh, X. Bu, B. Li, J. Liu, G.J. Freeman, M.A. Brown, K.W. Wucherpfennig, X.S. Liu, Signatures of T cell dysfunction and exclusion predict cancer immunotherapy response, Nat. Med. 24 (10) (2018) 1550–1558, https://doi.org/10.1038/s41591-018-0136-1.

[20] P. Geeleher, N. Cox, R.S. Huang, pRRophetic: an R package for prediction of clinical chemotherapeutic response from tumor gene expression levels, PLoS One 9 (9) (2014) e107468, https://doi.org/10.1371/journal.pone.0107468.

[21] K.J. Livak, T.D. Schmittgen, Analysis of relative gene expression data using real-time quantitative PCR and the 2(-Delta Delta C(T)) Method, Methods 25 (4) (2001) 402–408, https://doi.org/10.1006/meth.2001.1262.

[22] P. Bardou, J. Mariette, F. Escudié, C. Djemiel, C. Klopp, jvenn: an interactive Venn diagram viewer, BMC Bioinf. 15 (1) (2014) 293, https://doi.org/10.1186/1471-2105-15-293.

[23] N.N. Pavlova, C.B. Thompson, The emerging hallmarks of cancer metabolism, Cell Metabol. 23 (1) (2016) 27–47, https://doi.org/10.1016/j.cmet.2015.12.006.

[24] J.E. Trosko, On the potential origin and characteristics of cancer stem cells, Carcinogenesis 42 (7) (2021) 905–912, https://doi.org/10.1093/carcin/bgab042.

[25] A. Garten, S. Schuster, M. Penke, T. Gorski, T. de Giorgis, W. Kiess, Physiological and pathophysiological roles of NAMPT and NAD metabolism, Nat. Rev. Endocrinol. 11 (9) (2015) 535–546, https://doi.org/10.1038/nrendo.2015.117.

[26] H. Yang, S.M. Lee, B. Gao, J. Zhang, D. Fang, Histone deacetylase sirtuin 1 deacetylates IRF1 protein and programs dendritic cells to control Th17 protein differentiation during autoimmune inflammation, J. Biol. Chem. 288 (52) (2013) 37256–37266, https://doi.org/10.1074/jbc.M113.527531.

[27] J. Galon, A. Costes, F. Sanchez-Cabo, A. Kirilovsky, B. Mlecnik, C. Lagorce-Pagès, M. Tosolini, M. Camus, A. Berger, P. Wind, F. Zinzindohoué, P. Bruneval, P. H. Cugnenc, Z. Trajanoski, W.H. Fridman, F. Pagès, Type, density, and location of immune cells within human colorectal tumors predict clinical outcome, Science 313 (5795) (2006) 1960–1964, https://doi.org/10.1126/science.1129139.

[28] S. Yuan, P. Wang, X. Zhou, J. Xu, S. Lu, Y. Chen, Y. Zhang, Differential proteomics mass spectrometry of melanosis coli, Am J Transl Res 12 (7) (2020) 3133–3148.

[29] Y. Peng, Z. Zhang, A. Zhang, C. Liu, Y. Sun, Z. Peng, Y. Liu, Membrane-cytoplasm translocation of annexin A4 is involved in the metastasis of colorectal carcinoma, Aging (Albany NY) 13 (7) (2021) 10312–10325, https://doi.org/10.18632/aging.202793.

[30] M. Koslowski, U. Sahin, K. Dhaene, C. Huber, O. Türeci, MS4A12 is a colon-selective store-operated calcium channel promoting malignant cell processes, Cancer Res. 68 (9) (2008) 3458–3466, https://doi.org/10.1158/0008-5472.Can-07-5768.

[31] M. Koslowski, O. Türeci, C. Huber, U. Sahin, Selective activation of tumor growth-promoting Ca2+ channel MS4A12 in colon cancer by caudal type homeobox transcription factor CDX2, Mol. Cancer 8 (2009) 77, https://doi.org/10.1186/1476-4598-8-77.

[32] M.E. Loewen, G.W. Forsyth, Structure and function of CLCA proteins, Physiol. Rev. 85 (3) (2005) 1061–1092, https://doi.org/10.1152/physrev.00016.2004.

[33] I. Van der Auwera, W. Yu, L. Suo, L. Van Neste, P. van Dam, E.A. Van Marck, P. Pauwels, P.B. Vermeulen, L.Y. Dirix, S.J. Van Laere, Array-based DNA methylation profiling for breast cancer subtype discrimination, PLoS One 5 (9) (2010) e12616, https://doi.org/10.1371/journal.pone.0012616.

[34] M. Tusseau, E. Lovšin, C. Samaille, R. Pescarmona, A.L. Mathieu, M.C. Maggio, V. Selmanović, M. Debeljak, A. Dachy, G. Novljan, A. Janin, L. Januel, J. B. Gibier, E. Chopin, I. Rouvet, D. Goncalves, N. Fabien, G.I. Rice, G. Lesca, A. Labalme, P. Romagnani, T. Walzer, S. Viel, M. Perret, Y.J. Crow, T. Avčin, R. Cimaz, A. Belot, DNASE1L3 deficiency, new phenotypes, and evidence for a transient type I IFN signaling, J. Clin. Immunol. 42 (6) (2022) 1310–1320, https://doi.org/10.1007/s10875-022-01287-5.

[35] J. Chen, J. Ding, W. Huang, L. Sun, J. Chen, Y. Liu, Q. Zhan, G. Gao, X. He, G. Qiu, P. Long, L. Wei, Z. Lu, Y. Sun, DNASE1L3 as a novel diagnostic and prognostic biomarker for lung adenocarcinoma based on data mining, Front. Genet. 12 (2021) 699242, https://doi.org/10.3389/fgene.2021.699242.

[36] J. Liu, J. Yi, Z. Zhang, D. Cao, L. Li, Y. Yao, Deoxyribonuclease 1-like 3 may be a potential prognostic biomarker associated with immune infiltration in colon cancer, Aging (Albany NY) 13 (12) (2021) 16513–16526, https://doi.org/10.18632/aging.203173.

[37] G.G. Grassi, Clinical aspects of the relationship between antibiotic usage and resistance, J. Antimicrob. Chemother. 3 (Suppl C) (1977) 77–84, https://doi.org/10.1093/jac/3.suppl_c.77.

[38] B. Li, Y.Z. Ge, W.W. Yan, B. Gong, K. Cao, R. Zhao, C. Li, Y.W. Zhang, Y.H. Jiang, S. Zuo, DNASE1L3 inhibits proliferation, invasion and metastasis of hepatocellular carcinoma by interacting with β-catenin to promote its ubiquitin degradation pathway, Cell Prolif. 55 (9) (2022) e13273, https://doi.org/10.1111/cpr.13273.

[39] J. Sun, X. Wang, Q. Shen, M. Wang, S. Chen, X. Zhang, Y. Huang, Z. Zhang, W. Li, Y. Yuan, Z. Huang, DNASE1L3 inhibits hepatocellular carcinoma by delaying cell cycle progression through CDK2, Cell. Oncol. 45 (6) (2022) 1187–1202, https://doi.org/10.1007/s13402-022-00709-1.
[40] W. Li, H. Nakano, W. Fan, Y. Li, P. Sil, K. Nakano, F. Zhao, P.W. Karmaus, S.A. Grimm, M. Shi, X. Xu, R. Mizuta, D. Kitamura, Y. Wan, M.B. Fessler, D.N. Cook, I. Shats, X. Li, L. Li, DNASE1L3 enhances antitumor immunity and suppresses tumor progression in colon cancer, JCI Insight 8 (17) (2023), https://doi.org/10.1172/jci.insight.168161.
[41] L.J. Vuga, J. Milosevic, K. Pandit, A. Ben-Yehudah, Y. Chu, T. Richards, J. Sciurba, M. Myerburg, Y. Zhang, A.V. Parwani, K.F. Gibson, N. Kaminski, Cartilage oligomeric matrix protein in idiopathic pulmonary fibrosis, PLoS One 8 (12) (2013) e83120, https://doi.org/10.1371/journal.pone.0083120.
[42] F. Magdaleno, E. Arriazu, M. Ruiz de Galarreta, Y. Chen, X. Ge, L. Conde de la Rosa, N. Nieto, Cartilage oligomeric matrix protein participates in the pathogenesis of liver fibrosis, J. Hepatol. 65 (5) (2016) 963–971, https://doi.org/10.1016/j.jhep.2016.06.003.
[43] H. Ma, Q. Qiu, D. Tan, Q. Chen, Y. Liu, B. Chen, M. Wang, The cancer-associated fibroblasts-related gene COMP is a novel predictor for prognosis and immunotherapy efficacy and is correlated with M2 macrophage infiltration in colon cancer, Biomolecules 13 (1) (2022), https://doi.org/10.3390/biom13010062.
[44] Q. Li, C. Wang, Y. Wang, L. Sun, Z. Liu, L. Wang, T. Song, Y. Yao, Q. Liu, K. Tu, HSCs-derived COMP drives hepatocellular carcinoma progression by activating MEK/ERK and PI3K/AKT signaling pathways, J. Exp. Clin. Cancer Res. 37 (1) (2018) 231, https://doi.org/10.1186/s13046-018-0908-y.
[45] A.M. Blom, C. Gialeli, C. Hagerling, J. Berntsson, K. Jirström, K.S. Papadakos, Expression of Cartilage Oligomeric Matrix Protein in colorectal cancer is an adverse prognostic factor and correlates negatively with infiltrating immune cells and PD-L1 expression, Front. Immunol. 14 (2023) 1167659, https://doi.org/10.3389/fimmu.2023.1167659.
[46] O. Dakhova, D. Rowley, M. Ittmann, Genes upregulated in prostate cancer reactive stroma promote prostate cancer progression in vivo, Clin. Cancer Res. 20 (1) (2014) 100–109, https://doi.org/10.1158/1078-0432.Ccr-13-1184.